The Charge and Potential Distributions at the Zinc Oxide Electrode

By J. F. DEWALD

(Manuscript received August 20, 1959)

Capacitance measurements made on single crystal zinc oxide electrodes in contact with aqueous electrolytes are reported. Over a wide range of bias and bulk donor density, the results are in almost quantitative accord with predictions of the simple Poisson-Boltzmann (Poisson-Fermi in the degenerate case) equation. This is shown to imply the complete absence of surface-state effects in this system. A very sharp discontinuity in the flat-band potential is observed at bulk electron densities in the range from 0.6 $\times$ 10^{18} to 2 $\times$ 10^{18} cm^{-3}. This and other effects, arising under varying surface treatments, are discussed in some detail. The use of the semiconductor/electrolyte interface in studying the properties of low-lying donors is illustrated for the case of boron, which is shown to lie about 0.3 ev below the conduction band.

I. INTRODUCTION

The modern era in the study of the semiconductor electrolyte interface dates back to Brattain and Garrett's work[1] on the germanium electrode. Practically all of the studies since that time have been on germanium, this work being summarized in two recent review articles.[2,3] Although the qualitative understanding of the germanium electrode is fairly well advanced, complications arise because of the chemical reactivity of the material. This leads, in aqueous solutions at least, to the presence of oxide films and, in addition, precludes study of the electrode under equilibrium conditions.*

Zinc oxide was chosen for the present study because, of all the thermodynamically stable semiconductors (in contact with aqueous solutions), its bulk properties (band structure, mobilities, impurity ionization energies, etc.) are now the most thoroughly understood. We are concerned in the present paper with the distributions of charge and potential at the zinc oxide electrolyte interface.

* See, for example, the work of Bohnenkamp and Engel.[4]

Fig. 1 shows a diagram of a typical n-type semiconductor electrode in contact with an electrolyte under conditions of anodic bias (bands bending up). The conventional energy-band diagram for the system is also shown in Fig. 1. In general, the Galvani (or inner) potential difference, ψ_0, may distribute itself over three regions of the interface: (a) the space-charge layer in the semiconductor, typically 10^{-4} cm or more thick; (b) the one or two atom-diameter region of the Helmholtz layer; (c) the diffuse Gouy layer in the electrolyte. Since the Gouy layer has been much investigated in studies of metal electrodes and is no different at a semiconductor electrode, we will restrict ourselves in both our experimental and theoretical treatments to conditions (namely high ionic concentration in the electrolyte) under which the potential drop across the Gouy layer is negligible. The potential drop across the space-charge layer in the semiconductor, ψ_s, is called the *surface potential.*

The nature of the charge and potential distributions has been determined by measuring the differential capacitance of the zinc oxide electrode as a function of bias. The methods used are identical in principle to those which have been used with metal electrodes to distinguish

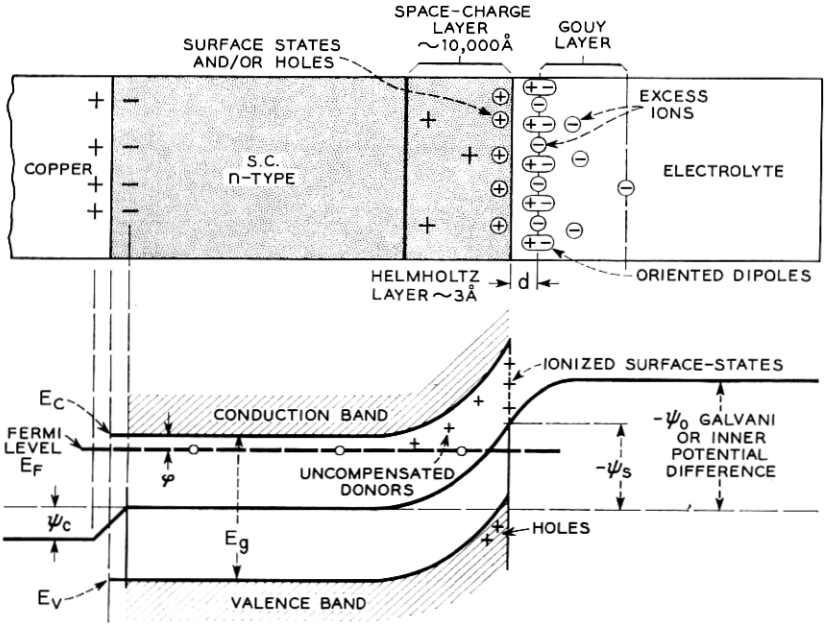

Fig. 1 — Schematic structure and energy-level diagram of a typical n-type semiconductor/electrolyte interface. By convention, one takes the potential in the bulk of the semiconductor to be zero, using the center of the gap as reference point.

"specifically adsorbed" charge residing in the Helmholtz layer from the charge in the Gouy layer.[5] Using the nomenclature of Fig. 1, the capacitance, C, of the electrode may be written*

$$C = -\frac{dQ}{d\psi_0} = -\left(\frac{dQ_{sc}}{d\psi_s} + \frac{dQ_{ss}}{d\psi_s}\right)\frac{d\psi_s}{d\psi_0}, \tag{1}$$

where Q, Q_{sc} and Q_{ss} are, respectively, the total charge on the semiconductor, the charge in the space-charge layer and the charge in "surface states."† For the assumed condition of a negligible potential drop across the Gouy layer, there may still be a sizable variation of the potential drop across the Helmholtz layer if the surface-state density is large. This potential drop may be estimated by taking

$$\frac{d\psi_s}{d\psi_0} = 1 - \frac{C}{C_H}, \tag{2}$$

where C_H is the capacitance of the Helmholtz layer, which should be of the same order of magnitude as that at a metal electrode ($\sim$30 μf/cm^2 on mercury)[5] and thus, anticipating our experimental results, very much larger than C over the entire range of potentials studied. Equations (1) and (2) may thus be combined to yield

$$C = -\left\{\frac{dQ_{sc}}{d\psi_s} + \frac{dQ_{ss}}{d\psi_s}\right\}\left(1 - \frac{C}{C_H}\right) \approx -\left(\frac{dQ_{sc}}{d\psi_s} + \frac{dQ_{ss}}{d\psi_s}\right). \tag{3}$$

This may be written in the form

$$\frac{1}{C} = \frac{1}{C_H} + \frac{1}{C_{sc} + C_{ss}}, \tag{4}$$

where C_{sc} and C_{ss} — in effect, capacitances of the space-charge layer and of the surface states — are defined respectively as $dQ_{sc}/d\psi_s$ and $dQ_{ss}/d\psi_s$.

* Unfortunately, the surface physicist's convention for the sign of potentials is not the same as that of the electrochemist. The physicist says that the more the bands bend up, i.e., the more anodic the bias, the more *negative* is the surface potential. The electrochemist says that the more anodic the bias, the more *positive* the electrode potential. We shall use *both* conventions, according to the context of the statement involved, using unambiguous phrases such as "anodic," "cathodic," "bands bent up," "bands bent down" when confusion is particularly probable.

† Surface-states on a semiconductor were first invoked by Bardeen[6] in an attempt to understand the fact, determined from field-effect conductivity measurements, that the electric field did not penetrate as far into the semiconductor as simple theory said it should. In effect, surface states are analogous to "specifically adsorbed" charge at a metal electrode. The major difference is that surface states equilibrate with the *electrode* rather than with the electrolyte. Law[7] gives a review of recent work on surface states. For a given crystal and surface condition, Q_{ss} is assumed to be uniquely determined by ψ_s .

With these definitions, (4) shows that the total capacitance may be represented by an equivalent circuit with a capacitance C_H in series and two capacitances, C_{sc} and C_{ss}, in parallel. Now C_{sc} may be computed from first principles (see below) and C_H estimated from results with metal electrodes, so that a measurement of C gives an estimate of C_{ss}.

II. THEORY OF THE SPACE-CHARGE CAPACITANCE FOR A SINGLE IMMOBILE DONOR

The theory of the space-charge layer at a semiconductor surface has been given by a number of workers.[8,9,10] We derive here the space-charge capacitance for the case of a large-energy-gap n-type semiconductor with immobile donors that may, however, be only partially ionized. A number of our crystals contained low-lying donors, and the results are understandable only in terms of this more elaborate treatment, which includes strongly dissociated donors as a special case. The Poisson-Boltzmann equation is used, consideration of the degenerate surface being given in a separate treatment below. The situation here is quite analogous to that existing in the Gouy layer with the one exception that one of the charged species is immobile.*

The Poisson-Boltzmann equation for the system may be written

$$\frac{d^2y}{dx^2} = \frac{q^2}{\kappa\epsilon_0 kT}(n_0 e^y - N^+), \tag{5}$$

where n_0 is the electron density in the bulk of the semiconductor, N^+ is the density of *ionized* donors at the point x (measured from the surface) and y is the potential, measured from the bulk, in units of kT/q. This assumes that the electrons are in equilibrium all across the space-charge layer and that, because of the large energy gap, the space charge due to holes is negligible. We also assume that at each point the donor ionization reaction

$$M \leftrightharpoons M^+ + e^- \tag{6}$$

is in equilibrium with the *local* electron density (ne_0^y). The equilibrium constant, K, for this reaction may be written in the form[12]

$$\frac{nN^+}{N_D - N^+} = N_c\left[\frac{m^{(N)}}{m}\right]^{\frac{3}{2}} D^{-1} \exp\left(\frac{-E_D}{kT}\right) = K, \tag{7}$$

where N_D is the *total* density of donors, N_c is the free electron density-of-states $[2(2mkT/h^2)^{\frac{3}{2}}]$, m is the electron mass, $m^{(N)}$ is the density-of-states effective mass, D is the donor degeneracy, and E_D is the energy

* Macdonald[11] has treated this problem previously. [Note added in proof.]

difference between the donor level and the bottom of the conduction band.

K and N_D are constant across the space-charge layer. However, because of the electric field, the electron density (n) and the *ionized* donor density (N^+) vary in a manner consistent with (7). Inserting (7) into (5), integrating once with respect to y, and using the boundary condition that in the bulk of the crystal y and dy/dx are both zero, we obtain the electric field at any point, x, in the form

$$\frac{dy}{dx} = \pm \left(\frac{2q^2N_D}{\kappa\epsilon_0 kT}\right)^{\frac{1}{2}} \{f(e^y - 1) - y + \ln[f + (1 - f)e^y]\}^{\frac{1}{2}}, \quad (8)$$

where

$$f = \frac{N_0^+}{N_D};$$

i.e., f is the fraction of the donors that are ionized in the bulk of the semiconductor. The positive sign in (8) applies when the bands bend up, the negative sign when they bend down.

Now the space-charge capacitance is the derivative of the space charge, Q_{sc}, with respect to the surface potential, with Q_{sc} in turn being given by

$$Q_{sc} = \kappa\epsilon_0 \frac{kT}{q} \left(\frac{dy}{dx}\right)_{x=0}. \quad (9)$$

The space-charge capacitance is obtained by substituting (8) into (9) and differentiating:

$$C_{sc} = -\frac{dQ_{sc}}{d\psi_s} = \left(\frac{q^2N_D\kappa\epsilon_0}{2kT}\right)^{\frac{1}{2}} \frac{\left| fe^Y - \dfrac{1}{1 + \left(\dfrac{1}{f} - 1\right)e^Y} \right|}{\{f(e^Y - 1) - Y + \ln[f + (1 - f)e^Y]\}^{\frac{1}{2}}}, \quad (10)$$

where Y is the value of the surface potential in units of kT/q, i.e., the value of y at $x = 0$. If the donors are completely ionized in the bulk of the semiconductor, $f = 1$ and (10) reduces to

$$C_{sc} = \left(\frac{q^2N_D\kappa\epsilon_0}{2kT}\right)^{\frac{1}{2}} \frac{|e^Y - 1|}{\{e^Y - Y - 1\}^{\frac{1}{2}}}. \quad (11)$$

A number of special cases of (10) are of specific interest. When Y is strongly negative; i.e., when the bands are bent up quite strongly, we have

$$C_{sc} = \left(\frac{q^2N_D\kappa\epsilon_0}{2kT}\right)^{\frac{1}{2}} \{-f + \ln f - Y\}^{-\frac{1}{2}}. \quad (12)$$

In the limit of large negative Y this is just the Mott-Schottky approximation.[8,9] Independent of the value of f, a plot of $1/C_{sc}^2$ versus Y should give a straight line, at sufficiently negative Y, whose slope is a measure of the *total* donor density at the surface. The only implied requirement is that the electrons be in equilibrium across the space-charge layer, i.e., that the Fermi level be flat right up to the surface. The maximum value by which the bands can be bent up while still keeping the Fermi level flat depends upon the magnitude of the current flow across the semiconductor/electrolyte interface. While this may be very small (less than 10^{-10} amperes/cm^2 in typical experiments on zinc oxide), it is still finite, and in consequence the Fermi level, under increasing anodic bias, eventually starts to follow the bands. At best, (12) is expected to apply for donors located less than one volt or so below the Fermi level.

At the other extreme of potential, when the bands bend down and Y is large and positive, (10) may be approximated in the form

$$C_{sc} = \left(\frac{q^2 N_D \kappa \epsilon_0}{2kT}\right)^{\frac{1}{2}} (fe^Y)^{\frac{1}{2}}. \tag{13}$$

As can be seen, the capacitance increases, apparently without limit, as the bands bend down, and the electrons tend to crowd up closer and closer to the surface. Eventually, however, the surface layers become degenerate and then the Poisson-Boltzmann approximation breaks down. This region is considered in greater detail below. The behavior of (10) in the region of intermediate potential is fairly complex, particularly for small values of f, and is also considered below.

III. EXPERIMENTAL PROCEDURES

3.1 *Sample Preparation*

The crystals used in this study were grown in these laboratories by D. G. Thomas and R. T. Lynch using the vapor-phase reaction between zinc and oxygen at about 1200°C, as originally reported by Scharowsky.[13] The resulting crystals were in the form of hexagonal needles, about 0.1 to 0.3 mm in "diameter" with the primary faces being {11.0}. Conductivities of the "as-grown" crystals were in the range from about 0.01 to 3.0 ohm^{-1} cm^{-1}. The crystals were selected for uniformity of composition, both lengthwise and radial. The lengthwise uniformity was checked by conductivity measurement, while the radial uniformity was checked by measurement of both conductivity and electrode capacitance between successive etches in 85 per cent H_3PO_4. Of a number of etching solu-

tions employed* this was found to be the most satisfactory by virtue of its uniform attack and its convenient rate (~1 micron per minute at room temperature).

In the lowest region of conductivity the crystals were used in the as-grown condition. For conductivities in excess of about 1 ohm^{-1} cm^{-1}, the crystals were "doped" by high-temperature diffusion of either hydrogen or indium into the crystal. Although it is the more convenient donor because of its higher diffusion coefficient,[14] hydrogen was not used extensively, since it was found to be too mobile, even at room temperature, under the very high electric fields near the surface.

Most of the crystals were doped with indium in a manner similar to that described by Thomas.[15]† For conductivities in excess of about 15 ohm^{-1} cm^{-1}, the crystals were equilibrated with an excess of $In(NO_3)_3$ (applied by dipping the crystal into an aqueous solution) at various temperatures in the range from 950° to 1150°C for periods up to about 20 days.‡ The crystals become saturated with respect to indium, the concentration depending upon the particular temperature selected. This procedure was rather tedious for conductivities below about 10 ohm^{-1} cm^{-1} because of the extended equilibration times that would have been required by virtue of the low temperatures. In this conductivity range the crystals were partially equilibrated with an excess of $In(NO_3)_3$ until the average conductivity had the desired value. The excess indium was then removed by etching in H_3PO_4, and the crystals were replaced in the oven, usually at 1100°C, for times calculated (from Thomas' diffusion data[15]) to give a maximum radial variation of no more than 20 per cent in donor density.

For some reason (not understood at present) a sizable fraction of the crystals treated in this manner showed very large radial nonuniformity, variations in conductivity as large as a factor of ten being not uncommon. Extending the equilibration time by factors of ten or more did not improve matters, the average conductivity increasing while the nonuniformity remained large. Other crystals, however, behaved quite nicely in accord with Thomas' diffusion data and, except for a surface skin about

---

* Other etches employed included HF, HNO_3 (both dilute and concentrated), HCl and KCN. The KCN etch is unique in developing quite nice {21.0} crystal faces even though one starts with {11.0} faces initially; H_3PO_4 preserves the original orientation.

† The indium ions enter the crystal substitutionally with an activation-energy-for-diffusion of about 3 ev compared to an activation energy of about 0.9 ev for the interstitial hydrogen.[14,15] Consequently, they are much less mobile.

‡ The oven employed was platinum-wound and had a recrystallized alumina lining to try to minimize contamination. The crystals were supported on other crystals of zinc oxide contained in "boats" of recrystallized alumina.

a micron thick, could be readily equilibrated. The only explanation of these effects that seems at all possible is that the indium diffusion is structure-sensitive (e.g., due to a varying dislocation density) and that a second donor (perhaps oxygen vacancies) is introduced when one equilibrates for times much in excess of the values calculated from Thomas' data. Whatever the cause of this effect, only those crystals were used that showed less than a 50 per cent variation in donor density over the entire crystal. The electron and donor densities reported below are appropriate averages.

Mechanically strong ohmic contacts were made to the crystals by electroplating a thin layer of indium on the tip of the crystal, then electroplating a second layer of copper on top of the indium and, finally, soldering a copper wire to the copper plate. A fairly large "glob" of solder was used, which completely surrounded the tip of the crystal. This clamps the crystal so tightly that, on an attempt to break the contact, the crystal breaks instead. The resistance of the contact was negligible compared to the crystal resistance over the entire range of conductivity from about 0.005 to 150 ohm^{-1} cm^{-1}.*

The solder joint and copper wire were masked by slipping the copper wire through a pyrex glass tube and then sealing with Apiezon W wax. The efficacy of the masking procedure was checked by measuring the direct current flow under anodic bias up to about 10 volts. If any of the copper, solder or indium is exposed to the solution, catastrophic currents flow under such a bias. On the other hand, a properly masked crystal passes anodic currents only of the order of 10^{-9} amperes per cm^2 or less, almost completely independent of the crystal resistivity.†

3.2 *Electrochemical Cell and Capacitance Bridge*

The electrochemical cell employed was of fairly standard design. It was made of quartz and contained a large-area working electrode of platinized platinum, a normal calomel electrode separated from the main solution by a 1 normal KCl salt bridge, and a second platinum electrode for preelectrolysis. A nitrogen atmosphere was maintained over the solution at all times. The solution was a borate-buffered 1 normal solution of recrystallized KCl (pH $\sim$ 8.5). Freshly ground, spectroscopically pure

* A more convenient but less satisfactory technique for making contact was to fuse a platinum wire directly to the crystal. This gives a nice low-resistance contact of good mechanical strength. However, the high temperature involved introduces impurities of an unknown nature and many of the results with such contacts were anomalous, particularly on crystals that were heat-treated subsequent to the platinum fusion.

† A study of the electrode kinetics at the zinc oxide electrode has been reported on[16] and details will be published shortly.

zinc oxide with an estimated area of about 10,000 cm^2 was added to the solution as a "getter" for any surface-active impurities. Periodic additions of more zinc oxide were made.

Impedance measurements were made using a General Radio #716-C bridge with an auxiliary decade-capacitance box in parallel with the variable air capacitor of the bridge. A schematic diagram of the circuit is shown in Fig. 2. The capacitance of the zinc oxide electrode, C_x, was always less than about 0.3 μf. The platinum working electrode had an apparent area of about 10 cm^2, so that its capacitance was more than 10^3 times C_x and thus made a negligible contribution to the total capacitance.

The equivalent circuit for the zinc oxide electrode is shown schematically in Fig. 2 as a resistance and capacitance in series. This is appropriate for the highest conductivity crystals studied, where the resistance is small and arises primarily in the electrolyte. For lower conductivity

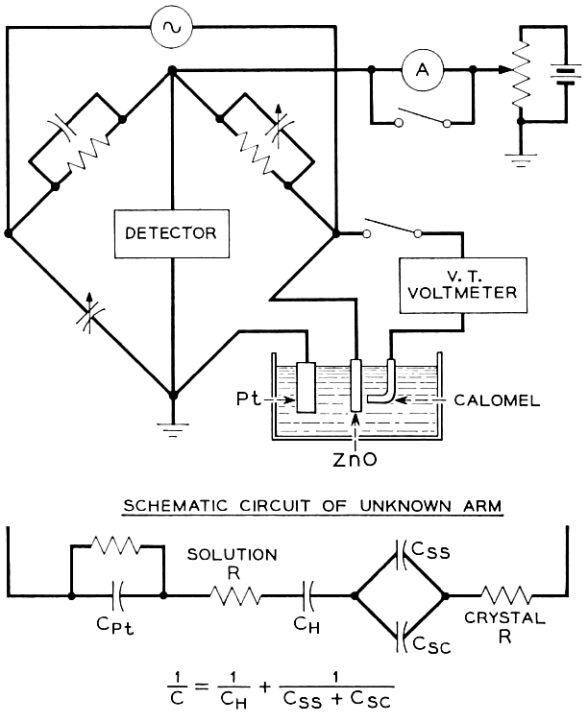

Fig. 2 — Schematic diagram of the capacitance bridge and the equivalent circuit of the unknown arm. The entire immersed area is in contact with the solution, Fig. 1 representing each *element* of area.

crystals the crystal resistance becomes predominant and sizable. Because of the rod-like habit of the crystals, the equivalent circuit is then analogous to a transmission line, the portions of the crystal nearest the tip having a larger resistance in series with them than do the regions near the metal contact. In most of the data presented below, the frequency was kept low enough to make the transmission-line correction negligible. Corrections, never over about 10 per cent, were made in the study of frequency effects.

The electrode bias applied to the crystal was varied potentiometrically and measured, with respect to the calomel electrode, by a Leeds and Northrup vacuum tube voltmeter with an impedance of 1600 megohms and a sensitivity of about ± 1 mv. The voltmeter was disconnected during capacitance measurement. The input signal to the bridge was kept below 10 mv. Measurements were made in the frequency range from 50 cps to 100 kc. The bridge was extensively calibrated at the start of the experiments, and then checked periodically during the course of the measurements. The major difficulty encountered was in the minimization of the lead capacitance, which was finally reduced to about 12 $\mu\mu$f. Even this small value was significant in the measurements of the lowest conductivity crystals, since the total capacitance in these crystals was as low as 150 $\mu\mu$f.

IV. EXPERIMENTAL RESULTS

4.1 *Exhaustion Region*

The results that have been obtained for the capacitance of the zinc oxide electrode in the exhaustion region, i.e., under anodic bias, are remarkable for their simplicity. The results for two crystals of intermediate conductivity are shown in Fig. 3. Here, taking our cue from (12), we plot the reciprocal of the capacitance squared against the electrode potential. As can be seen, the resulting plots are very nicely linear for the two crystals. This was the case for nearly every crystal studied; in only two crystals out of more than 50 was a curvature greater than 2 per cent observed in the region of positive potential (on the calomel scale).

The precision of the linearity on most crystals is quite remarkable and is illustrated in Table I for one of the crystals shown in Fig. 3. As can be seen, the slope is constant within about 0.5 per cent, the departures being well within the experimental uncertainty. This behavior is precisely that predicted for the Mott-Schottky space-charge capacitance [see (10)] and implies that the surface-state capacitance is very much smaller than the space-charge capacitance. Note in this connection that a capacitance versus bias curve for any *one* crystal can *always* be fitted

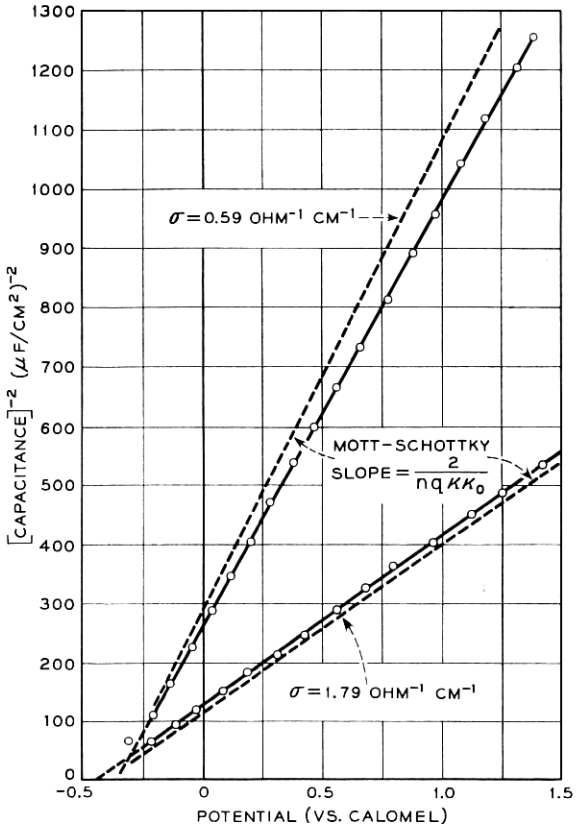

Fig. 3 — Mott-Schottky plots for two crystals under exhaustion conditions; the dotted lines represent the theoretical slopes. At potentials more negative than about −0.3 volt, the capacitance increases exponentially (see Fig. 8). The intercepts of the linear plots afford a quantitative measure of the electrode potential at the flat-band condition.

by a completely unrestricted distribution of surface states, such an interpretation violating only the law of simplicity. However, one cannot devise a single surface-state distribution that will simultaneously satisfy the results on crystals of varying impurity density.

The magnitude of the slope of the $1/C^2$ versus V plots confirms the simplicity of the results in the exhaustion region. Equation (12) says that, in the absence of surface states and if the donors are completely ionized (i.e., $N_D = n$), the slope should be given by

$$\text{slope} = \frac{2}{nq\kappa\epsilon_0}. \tag{14}$$

TABLE I — THE CAPACITANCE OF A TYPICAL CRYSTAL AS A FUNCTION OF BIAS

$\sigma = 0.59$ ohm^{-1}cm^{-1}

V_{cal}	Capacitance, C, in μf/cm^2	$1/C^2$	$\Delta\ 1/C^2$
1.400	0.02890	1197.3	
			253.5
1.000	0.03255	943.8	
			250.6
0.600	0.03798	693.2	
			252.4
0.200	0.04763	440.8	
			252.1
−0.200	0.07280	188.7	

Since the dielectric constant of zinc oxide is known[12] ($\kappa = 8.5$), the only unknown quantity is the electron density n, which can be obtained from conductivity and Hall-effect measurements. For the two crystals in Fig. 3 the agreement between the Mott-Schottky slope and the experimental slope is within experimental error,* as shown by the dotted lines whose slopes are calculated from (14).

In very good approximation the data are frequency independent, as shown for a typical case in Table II.

The conclusion that the surface-state capacitance is negligible compared to the space-charge capacitance is confirmed in all of our experiments. This is shown in Fig. 4, where we plot the slope of the $1/C^2$ versus V curves as a function of electron density. The open circles represent "as-grown" crystals, while the solid circles are for indium-doped samples. The straight line in Fig. 4 is an absolute prediction with no adjustable parameters. As can be seen, the agreement of the data with

TABLE II — THE FREQUENCY DEPENDENCE OF CAPACITY, CRYSTAL C-3

(Corrected for Transmission-Line Effect)

Frequency	Slope of $1/C^2$ vs. V Plot (μf^{-2}cm$^4V^{-1}$)	Flat-Band Potential*
100	626	−0.471
200	626	−0.471
1,000	628	−0.470
5,000	625	−0.483
10,000	629	−0.441

* See below.

* The major errors arise in the determination of surface area and in the determination that the crystals are in fact uniformly doped.

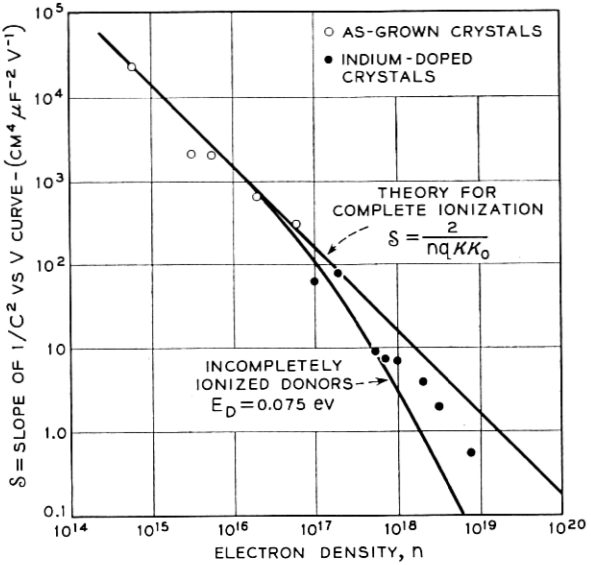

Fig. 4 — The Mott-Schottky slope as a function of the bulk electron density; the straight line is taken from (14) and represents a "no-parameter" fit to the data, the curved line shows the correction for incomplete donor dissociation with E_D = 0.075 ev.

this simple theory is fairly good over the entire range studied. It can be improved somewhat by realizing that at high density the indium donors are not completely ionized. Hutson's preliminary measurements[17] on indium donors indicate an ionization energy of about 0.075 ev at electron densities around 10^{17} or less. If we assume that this value applies over the entire range of concentration and use (7) with[12] $D = 2$ and $m^{(N)}/m = 0.5$, we obtain the curve marked "$E_D = 0.075$ ev." The data lie reasonably well between these extreme predictions.*

The experiments reported above show that the surface-state density is very low in the energy region up to about one volt below the conduction band. We may compute an order-of-magnitude upper limit for their number by considering the data obtained on the lowest conductivity crystal studied. The capacitance versus bias curve for this crystal agreed with that predicted for the simple space-charge layer capacitance within about 2 per cent over the entire exhaustion region. Thus, the total varia-

* The data from a number of crystals have been excluded from Fig. 4 owing to nonuniformity of the donor density. A few others which gave results widely discordant with those of Fig. 4 have also been excluded on the basis of a complex behavior at potentials in the range from 0 to −0.4 volts on the calomel scale. These effects are treated below and are shown to arise from the inadvertent introduction of boron which acts as a low-lying donor.

tion in the charge of the surface-states must have been less than about 2 per cent of the total space charge. The donor density in this crystal was about 0.7×10^{15}, so that the total charge in the space-charge layer [see (10)] at a surface potential of -0.7 volt was 7.7×10^{-9} coulombs/cm^2.* Two per cent of this corresponds to an upper limit for the surface-state density of the order of 10^{+9} states per cm^2, in the energy range from about 0.25 ev to 0.95 volt below the conduction band. (The Fermi level in this crystal lay about 0.25 ev below the conduction band.)

The effective absence of surface states at the zinc oxide/electrolyte interface implies that the electric field arising from free charge on the semiconductor cannot give rise to any significant potential drop across the Helmholtz layer. However, a variable potential drop across this layer can arise if desorbable polar molecules are present at the surface. A typical determination of a $1/C^2$ versus V plot normally took about 10 minutes. The nice linearity of these plots thus precludes any rapid changes with bias of the chemistry (and therefore the surface dipole) of the Helmholtz layer. Sizable slow changes of the surface dipole, on etching a crystal or on long-term equilibration, are indicated, however, by our measurements of the "flat-band potential," i.e., the electrode potential at which the bands are flat. At this potential the charge within the semiconductor is equal to zero.

The flat-band potential is a particularly important quantity with semiconductor electrodes. It is almost perfectly analogous to the potential of the electrocapillary maximum at metal electrodes. Two factors determine its magnitude (for a given reference electrode): the surface dipole at the electrolyte contact and the "built-in" potential drop at the ohmic contact to the lead wire. Both of these are subject to variation, the first by variation of the surface pretreatment and/or the nature of the solution, and the second by variation of the semiconductor doping. Since it is possible to make these variations independently, one can obtain information about both the surface dipole and the bulk Fermi level.

There are several methods of determining the flat-band potential. Surface-state effects having been shown to be absent, one can simply use (10) (in the limit as Y goes to zero) to compute the capacitance at flat band and then adjust the bias until this capacitance is attained. This method has the disadvantage that one must know the surface roughness of the crystal to go from capacitance per unit area, C_{sc}, to the total capacitance.

* The value of -0.7 volt is used here because, when the bands bend up much more than this, the Fermi level no longer remains flat and the surface states are no longer in equilibrium with the bulk Fermi level.

An alternative is to use (12). From this, we see that the extrapolation of the linear portion of a $1/C^2$ versus V plot to the voltage axis gives the potential at which the bands bend up by $(f - \ln f)(kT/q)$ volts. A knowledge of f then allows a computation of the flat-band potential, independent of any statements regarding surface roughness.

Fig. 5 shows the experimental variation of the flat-band potential (as determined by the second method described above), with the bulk electron density for three different surface treatments. The curves marked "H_3PO_4" and "KOH" were taken within a few minutes after a brief (2 to 10 second) etch-in for H_3PO_4 (85 per cent) and KOH (3M). The curve marked "long stand" was obtained with crystals that had stood in the buffered KCl electrolyte (pH $\sim$ 8.5) for 10 hours or more.

Consider the data at low concentration first. There are two possible sources of a variable flat-band potential: (a) a variable surface dipole and (b) a variable contact-potential difference at the copper/zinc oxide interface due to a variation in the bulk Fermi level. The latter variation goes as $(kT/q)\ln n$ for a nondegenerate semiconductor, and the straight lines at low electron density are drawn with slope to correspond to this variation (59 mv per decade in n). As can be seen, the change in the "built-in" potential at the copper/zinc oxide interface accounts for most,

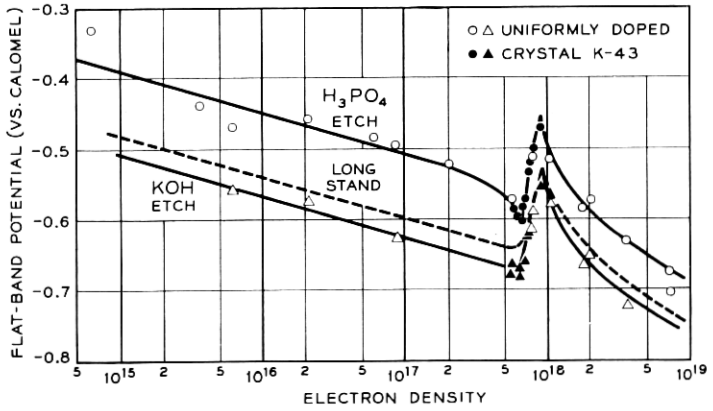

Fig. 5 — The variation of the flat-band potential with bulk electron density for three different surface treatments. The lines at low density are drawn with slope of 59 mv per decade, corresponding to the classical variation of the Fermi level with electron density. Each unshaded point represents a different crystal and/or a different surface treatment. The shaded points are the data obtained by successive etching of a crystal (K-43) containing a (purposely introduced) radial gradient of concentration. For these points the concentration is that just to the semiconductor side of the space-charge layer. The anomalous "bump" in the curves is thought to represent a similar discontinuity in Fermi level.

if not all, of the observed variation with crystal doping at levels below about 0.6×10^{18} electrons per cm^3. This is not particularly surprising, since the impurity density at such levels is quite low in normal chemical parlance (99.99 mole per cent ZnO) and one would not expect the chemistry of the surface to be strongly impurity-sensitive at these low levels.

A more physically interesting result is obtained from the variation of the flat-band potential with the nature of the surface treatment. As can be seen from Fig. 5, the flat-band potential becomes more negative by about 130 mv when one etches in KOH instead of H_3PO_4, corresponding to the addition of a surface dipole with the positive end towards the electrolyte (or removal of a dipole of opposite polarity). This effect is quite reproducible, on a given crystal, and quite rapid; a two-second etch in either H_3PO_4 or KOH (corresponding to the removal of about 300 Å and 30 Å in the two cases) brings the flat-band potential to the values shown, completely independent of the past surface treatment. Several crystals were cycled between acid and base as many as eight times, and the maximum deviation of the flat-band potential (for a given treatment) was about 15 mv. Other acids, HCl and HF for example, give the same value of the flat-band potential as H_3PO_4; however, they also roughen the surface appreciably and have therefore not been studied extensively.

The individual data points shown in Fig. 5 were obtained on freshly etched surfaces. If a crystal is allowed to stand in contact with the electrolyte, a slow change in flat-band potential is observed for upwards of five hours or more. The direction of the change depends upon the nature of the last previous etch, while the final limiting value of the flat-band potential is independent of the nature of the etch. Fig. 6 shows the typical transient behavior following a series of etches in H_3PO_4. Time

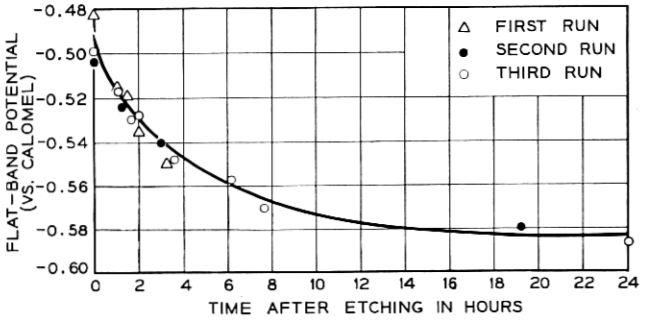

Fig. 6 — The variation of the flat-band potential with time after etching in H_3PO_4; various points correspond to three successive runs on same crystal.

constants for the effect are typically of the order of three hours, independent of crystal doping and also of the bias under which the crystal stands.

The 130-mv change in flat-band potential observed on going from a KOH-etched surface to an H_3PO_4-etched surface may be qualitatively understood as arising from a heterogeneous acid-base equilibrium. On an ideal {11.0} surface there are equal numbers of zinc and oxygen atoms in the surface plane. In the covalent model of the "clean" crystal surface each of these atoms has a "dangling" bond, while in the ionic structure each surface oxygen has an unshared pair of electrons pointing into the solution and each zinc has an empty pair of orbitals. The true situation is probably intermediate between these extremes, but in either case the oxygen will be able to accept a proton, becoming an OH^- ion, and the zinc will be able to complete its tetrahedral coordination by bonding with any ion or molecule from the solution that has an unshared pair of electrons.

A diagram of the surface structure expected when the {11.0} crystal face is in contact with a solution of HCl is shown in Fig. 7. Here we have drawn the zinc, oxygen and chloride atoms as if they were spheres of radius equal to Pauling's tetrahedral covalent radii, and the hydrogen is drawn as a sphere of radius sufficient to make the O–H distance equal to the bond length in the hydroxide ion (~1.0 Å). As can be seen, the proton gets much closer to the crystal than does the chloride ion. To the extent that the bonds have the same degree of ionic character — a not unreasonable approximation in view of the respective electronega-

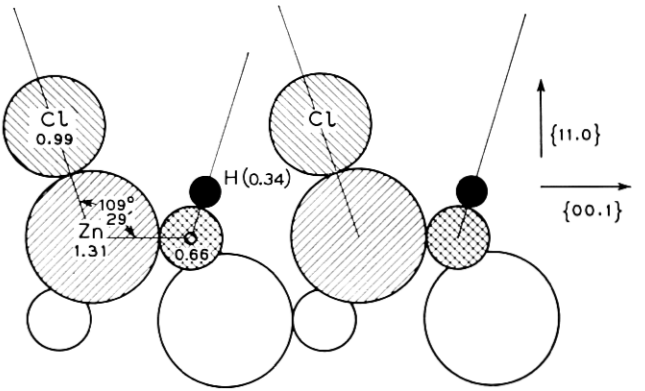

Fig. 7 — Diagram of the surface configuration on a {11.0} surface of ZnO in contact with a solution of HCl; the various distances are computed from Pauling's tetrahedral covalent radii.

tivities — this would then give a surface dipole with the negative side towards the solution. If such a surface is now treated with a strong base like KOH, the protons will tend to be removed, to be replaced by either water molecules or, conceivably, potassium ions. In either case, the surface dipole should become more negative. This is the direction of the change in flat-band potential observed on going from an acid to a basic etch. At intermediate values of pH we expect intermediate values of the flat-band potential corresponding to partial coverage of the surface with protons. This is qualitatively in accord with the data in Fig. 5, the flat-band potential at pH 8.5 being intermediate between the acid and basic treatments.

The one difficulty here is in understanding the very slow equilibration rate. The exchange of protons and chloride ions should presumably be quite rapid, and we cannot think of any other rate-limiting process. The large number of presently unverifiable assumptions involved (about electronegativity, dielectric saturation, etc.) makes it unprofitable to attempt a quantitative calculation of the size of the acid-base effect.

Consider now the data in Fig. 5 at high doping levels. A remarkably sharp "bump," amounting almost to a discontinuity, in the flat-band potential is observed centered at a bulk electron density of about 10^{18}, with the flat-band potential getting more *positive* by about 130 mv on going from an electron density of 0.6×10^{18} to 0.9×10^{18}. Within experimental error the contour of the bump is independent of surface treatment. The "width" of the bump is so small that in our early experiments, which had only one crystal in the range from 0.6×10^{18} to 3×10^{18}, we completely overlooked it and took the low-density behavior to be valid over the entire concentration range. We had then just a single anomalous point, which we rationalized as arising from some unknown anomaly in chemical or thermal history of the crystal. This rationalization became quite tenuous as further crystals were studied in this concentration range, and it was completely eliminated by the data shown as shaded points in Fig. 5. To obtain these data we took a crystal (K-43) that, from capacitance measurements, had a total donor density less than 10^{16} donors per cc and, by a relatively short heat treatment with indium, produced a nonuniform donor distribution. The outside of the crystal had a donor density near 10^{18}, while the inside was at a level around 10^{17} donors per cc. Capacitance and conductivity measurements were then made as the crystal was successively etched. In this way we obtained a plot of flat-band potential versus surface donor density with a minimum of ambiguity as regards uncontrolled variables of thermal and chemical nature. The results are shown in Table III and illustrated graphically in Fig. 5.

TABLE III — THE VARIATION OF THE FLAT-BAND POTENTIAL NEAR THE ANOMALOUS "BUMP", CRYSTAL K-43

Etch Time (minutes in H_3PO_4)	Crystal "Diameter" $= \left(\frac{4}{3} A_{cross}\right)^{\frac{1}{2}}$	Slope of $1/C^2$ vs. V plot*	Intercept in H_3PO_4	Intercept in KOH	Electron Density†
1	0.0238	8.45	−0.441	−0.524	8.7×10^{17}
2	—	9.81	−0.473	−0.559	7.8×10^{17}
3	—	10.30	−0.490	−0.588	7.50×10^{17}
4	—	10.60	−0.504	−0.593	7.25×10^{17}
6	—	11.16	−0.544	−0.630	6.90×10^{17}
8	—	11.89	−0.553	−0.632	6.60×10^{17}
10	—	12.45	−0.574	−0.639	6.40×10^{17}
15	—	12.86	−0.570	−0.656	6.20×10^{17}
25	0.0208	14.05	−0.556	−0.650	5.75×10^{17}
35	—	13.95	−0.563	−0.642	5.80×10^{17}

* On H_3PO_4-etched crystal.
† Electron densities computed from slope of $1/C^2$ vs. V plots using Fig. 4.

As can be seen, these data are nicely consistent with the data obtained on uniformly doped crystals and demonstrate, to our satisfaction at least, that the anomalous variation of flat-band potential with doping is a real effect.

We have no explanation of the anomaly at the present time. The value of the electron density at which it occurs would seem to be unique in one way, 10^{18} electrons per cc marking the onset of electronic degeneracy in zinc oxide. However, it is hard to see how this would play any role in determining the surface dipole. Another possible explanation is that the Fermi level is exhibiting an anomolous variation with impurity density. This would show up as an anomalous variation in the built-in potential difference at the zinc oxide/copper interface.

A few experiments have been made to see the effects of known impurities in the electrolyte upon the capacitance and flat-band potential. The addition of octyl alcohol, which is known to be strongly absorbed at a mercury electrode,[18] has no measurable effect on the capacitance over the entire range of potentials studied.* Nitrobenzene, a strongly polar molecule, was also found to have no effect on the capacitance. Further

* This is perhaps not too surprising on the anodic side of the flat-band potential since in Grahame's study[18] the *potential* of the electrocapillary maximum was not significantly affected by octyl alcohol but only the capacitance, which decreased from about 30 μf per cm^2 to about 4 μf per cm^2. It *is* surprising that no effect was observed at cathodic potentials (see Fig. 8). A comparable change in the capacitance of the Helmholtz layer at the zinc oxide electrode would have been readily detectable at bias 0.3 volt or more cathodic than the flat-band potential where the capacitance is of the order of 5 μf per cm^2.

study of these effects is surely warranted. For the present, we conclude that, although the free charge on the zinc oxide electrode is located almost entirely *inside* the semiconductor, significant portions of observed changes in electrode potential may still occur across the Helmholtz layer.

4.2 *Enrichment Region*

Consider now the data obtained in the enrichment region, i.e., when the bands are bent down. Results typical of the behavior of crystals with completely (or nearly completely) dissociated donors are shown in Fig. 8. As seen from (13), the simple Poisson-Boltzmann theory predicts an exponential dependence of capacitance on bias starting near the flat-band potential. For crystals of conductivity below about 1 ohm^{-1} cm^{-1},

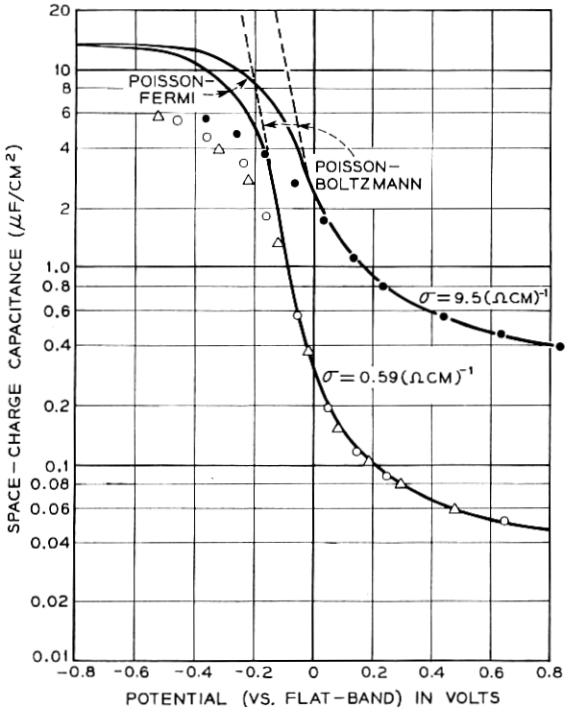

Fig. 8 — The capacitance versus bias curves for two typical crystals at potentials near and cathodic to the flat-band potential; the theoretical curves marked Poisson-Boltzmann and Poisson-Fermi involve only one unknown parameter, the flat-band potential, with is determined from plots like Fig. 3. At points indicated by triangles electrolyte contained a few drops of octyl alcohol.

such an increase is in fact observed in the potential region between where the bands are flat and where the conduction band at the surface goes degenerate.* However, with crystals of conductivity much higher than 1 ohm^{-1} cm^{-1} this region is so narrow as to make the limiting form of (13) invalid.

The curves labeled "Poisson-Boltzmann" in Fig. 8 were calculated from equation (10) and contain no new adjustable parameters. Sizable departure of the experimental data from the Poisson-Boltzmann predictions is observed when the potential is sufficiently negative to make the surface degenerate. An important point here is that all the experimental points lie, if anything, *below* the Poisson-Boltzmann curves. The presence of surface-states would cause departures in the opposite direction. A second feature of the data is that at sufficiently negative bias (~ -0.4 volt with respect to the flat-band potential) the capacitance becomes almost completely independent of the bulk electron density and appears to approach a limiting value of the order of 6 μf per cm^2 at the most negative potentials studied.

A large number of factors neglected in the derivation of (10) can operate to make the measured capacitance lower than the Poisson-Boltzmann values. For one thing, the capacitances of the Helmholtz and Gouy layers are in series with the space-charge capacitance, and it may be incorrect to use the value of 30 μf per cm^2 for C_H in obtaining the space-charge capacitance from the measured capacitance. This value was taken from work with the mercury electrode. Since the highest capacitance measured was about 6 μf per cm^2, it seems unlikely that this is the cause of the discrepancy. In this connection it should be noted that, if the surfaces were rough, any error in using too large a value for C_H would be partly compensated.

The most important effect causing the capacitance to fall below the Poisson-Boltzmann prediction is the onset of degeneracy at the surface. When the bands bend down sufficiently to make the Fermi level lie within the conduction band, the effective density-of-states treatment breaks down. Since only one electron can be put into each level and the number of levels at each energy is finite, the conduction-band electrons at the surface must have energies lying well into the conduction band. This counteracts the tendency of the electric field to pull electrons towards the surface, and makes the electron density at the surface less than that predicted from the classical treatment. In consequence, the capacitance is also less than classical.

* Degeneracy starts to be important when the Fermi level lies above the conduction band.

The effects of surface degeneracy may be treated quantitatively by the use of Fermi-Dirac statistics in conjunction with an effective mass approximation.[19] The electron density n at any point in the space-charge layer is then given by

$$n = \frac{2}{\sqrt{\pi}} N_c \left(\frac{m^{(N)}}{m}\right)^{\frac{3}{2}} \int_0^\infty \frac{\epsilon^{\frac{1}{2}}\, d\epsilon}{1 + e^{\epsilon+\varphi-y}}, \tag{15}$$

where N_c is the effective density-of-states [see (7)], $m^{(N)}$ is the density-of states mass and φ is the Fermi energy measured from the conduction band in the bulk of the crystal. ϵ and φ are in units of kT. When this expression is inserted in the Poisson equation, one may approximate the resulting integrals (within a few per cent or less if $Y - \varphi > 3$) and obtain the capacitance in the form.

$$C_{sc} = \left\{\frac{5\kappa\epsilon_0 N_c q^2}{3\pi^{\frac{1}{2}}kT}\left[\frac{m^{(N)}}{m}\right]^{\frac{3}{2}}\right\}^{\frac{1}{2}} (Y - \varphi)^{\frac{1}{4}}. \tag{16}$$

Using Hutson's[12] values for $m^{(N)}$ and κ, this becomes, at room temperature,

$$C_{sc} = 6.1(Y - \varphi)^{\frac{1}{4}} \qquad \mu\text{f per cm}^2. \tag{17}$$

The capacitance in this degenerate region depends upon bias only as the one-fourth power and depends almost negligibly upon the donor density (through φ). As the curves in Fig. 8 marked "Poisson-Fermi" show, the qualitative features of (17) are reasonably well in accord with the experimental result. This is particularly striking in view of the fact that no additional adjustable parameters are used in drawing the curves.

It is tempting to try to rationalize the quantitative discrepancy between the experimental data and (17). It could be due to using too high a value for C_H. Alternatively, the use of Hutson's value of 0.5 for the density-of-states mass, $m^{(N)}$, may not be valid, since we are concerned here with the density-of-states at the *surface* and Hutson's measurement was for the bulk. If anything the density of states near the surface should be less than that in the bulk. If the density-of-states mass near the surface were half the bulk value, the agreement between theory and experiment would be truly quantitative.

A more exact treatment than the Poisson-Fermi equation, presumably treating the electrons as quantum particles and including discreteness-of-charge effects, is probably required before any sound conclusions can be drawn from the discrepancy.

4.3 *Results with Boron and Hydrogen Donors*

The results presented above are typical of the majority of crystals that have been studied. Since they agree quite well with the simple

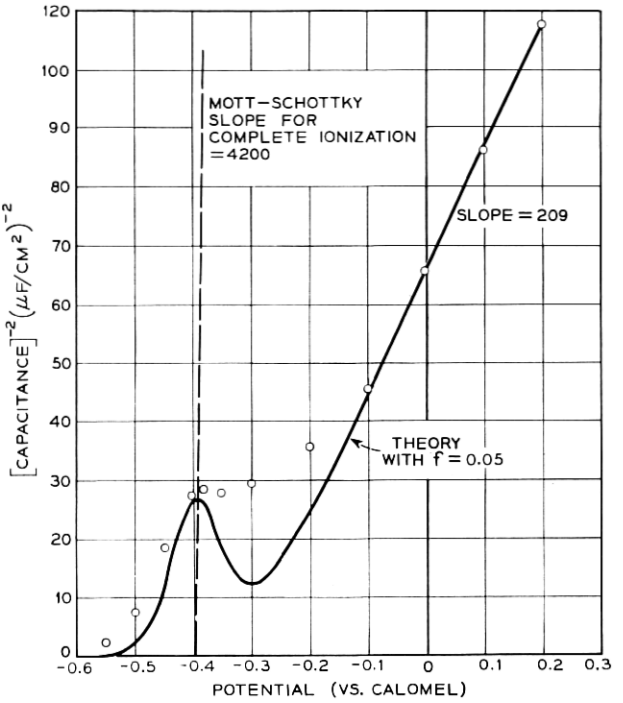

Fig. 9 — Mott-Schottky plot for a crystal containing boron, a low-lying donor; the dotted line shows the slope expected at this electron density if all the donors were ionized, solid line is the complete theory [equation (10)] if the donors are 5 per cent ionized.

theory outlined above, we are reasonably confident that they represent the "normal" behavior for crystals with a uniformly distributed immobile donor lying reasonably close to the conduction band. A number of "anomalous" types of behavior have also been observed. As we shall see, all but one of these anomalous results are understandable, in at least a qualitative fashion, as arising from donor inhomogeneity, donor mobility and/or weak donor ionization. They are presented here in the interest of completeness and also to illustrate the use of surface capacitance measurements in studying the bulk properties of semiconductors.

Fig. 9 shows the behavior typical of one lot of crystals into which boron was inadvertently introduced.* Here we plot $1/C^2$ versus bias as in Fig. 3. For positive potentials (versus calomel) the data were nicely linear as prediced by (12). However, the slope was only about one-twentieth of the value expected if all the donors were ionized, when the

* It was subsequently identified by spectral analysis.

conductivity and Hall effect results, indicating an electron density of about 3.9×10^{15}, would predict a Mott-Schottky slope of 4200 (μf per cm^2)$^{-2}$ volt^{-1}. This is shown by the dotted line in the figure. But the observed slope is only 209. Conductivity and capacitance measurements made after successive etching in H_3PO_4 indicated that the crystal was essentially uniform in composition (within 20 per cent or so) and ruled out the possibility of an excessive donor concentration near the surface. The simplest explanation of the much reduced Mott-Schottky slope in Fig. 9 is that the donors in the bulk of the crystal are only about one-twentieth ionized.

The dependence of capacitance on bias in the region of negative potentials is complex for this crystal. It confirms in at least a qualitative way the assumption of incomplete ionization. With increasingly negative bias, the theoretical capacitance computed from (10) goes through a maximum and then a minimum (located near the flat-band potential) before finally rising exponentially as predicted by (13).

The solid curve in Fig. 9 is computed for $f = 0.05$, this value being obtained from the slope at strongly positive potentials. As can be seen, the experimental data show behavior that is qualitatively similar to theory. The value of the capacitance at the minimum and also the potential at which it occurs are in good accord with the theory. The only discrepancy is that the capacitance maximum (the minimum in the curve as plotted) is very much shallower than predicted by (10). The reason for this is not presently understood. It might conceivably arise from the presence of two kinds of donors. However, curve fitting for such a situation, with the consequent introduction of two more parameters, does not seem waranted.

If one accepts the value of 0.05 for f, (6) allows one to compute the energy of the boron level in zinc oxide. Assuming a donor degeneracy of 2 and Hutson's value of 0.5 m for $m^{(N)}$, one obtains a value of 0.30 ev for E_D. This agrees quite well with a preliminary measurement by Zetterstrom[20] of the temperature dependence of Hall effect and conductivity which gave a value of 0.32 ev for E_D.

Hydrogen-doped crystals showed complicated frequency effects and long-term transients.

V. SUMMARY

i. The differential capacitance of single-crystal zinc oxide electrodes has been studies as a function of bias, frequency, surface treatment and crystal impurity content in the range from 10^{15} to 10^{19} ions per cc.

ii. Under nondegenerate surface conditions the results on "as-grown" and indium-doped crystals are quantitatively in accord with the capacitance calculated from the Poisson-Boltzmann equation, surface states playing no role whatsoever. Boron-doped crystals can also be understood in these terms if one assumes boron to be a low-lying donor.

iii. The variation of the flat-band potential with surface treatment indicates that a variable surface dipole is present. A strongly anomalous dependence of flat-band potential on donor density is observed at densities around 2×10^{18} donors per cc. It is speculated that this may be a direct measure of an anomalous variation in Fermi energy.

iv. Under conditions where the surface is degenerate, the results are in almost quantitative agreement with those predicted by the Poisson-Fermi equation.

VI. ACKNOWLEDGMENTS

I am indebted to J. J. Lander and A. R. Hutson for many stimulating discussions of this work. I am also indebted to R. T. Lynch, who grew most of the crystals used. I am particularly appreciative of the efforts of R. B. Zetterstrom, who made all of the Hall-effect measurements.

REFERENCES

1. Brattain, W. H. and Garrett, C. G. B., B.S.T.J., **34,** 1955, p. 129.
2. Dewald, J. F., in Hannay, B. N., ed., *Semiconductors*, Reinhold Publishing Corp., New York, 1959, p. 727.
3. Green, M., in Bockris, J. O., ed., *Modern Aspects of Electrochemistry, No. 2*, Academic Press, New York, 1959.
4. Bohnenkamp, K. and Engell, H. J., Z. Elektrochem., **61,** 1958, p. 1184.
5. Parsons, R., in Bockris, J. O., ed., *Modern Aspects of Electrochemistry, No. 1*, Academic Press, New York, 1954.
6. Bardeen, J., Phys. Rev., **71,** 1947, p. 717.
7. Law, J. T., in Hannay, N. B., ed., *Semiconductors*, Reinhold Publishing Corp., New York, 1959, p. 676.
8. Schottky, W., Z. Physik, **113,** 1939, p. 367; **118,** 1942, p. 539.
9. Mott, N. F., Proc. Royal Soc., **A171,** 1939, p. 27.
10. Garrett, C. G. B. and Brattain, W. H., Phys. Rev., **99,** 1955, p. 376.
11. Macdonald, J. R., J. Chem. Phys., **29,** 1958, p. 1346.
12. Hutson, A. R., Phys. Rev., **108,** 1957, p. 222.
13. Scharowsky, E., Z. Physik, **135,** 1953, p. 318.
14. Thomas, D. G. and Lander, J. J., J. Chem. Phys., **25,** 1956, p. 1136.
15. Thomas, D. G., J. Phys. Chem. Solids, **9,** 1958, p. 31.
16. Dewald, J. F., Abst. New York Meeting, Amer. Electrochem. Soc., 1958.
17. Hutson, A. R., private communication.
18. Grahame, D. C., J. Am. Chem. Soc., **68,** 1946, p. 301.
19. Hannay, N. B., *Semiconductors*, Reinhold Publishing Corp., New York, 1959, p. 13.
20. Zetterstrom, R. B., private communication.